Journal of Achievements in Materials and Manufacturing Engineering
VOLUME 33
ISSUE 2
April
2009

Simplified and advanced models of a valve system used in shock absorbers

P. Czop [a,*], D. Sławik [a], P. Śliwa [a], G. Wszołek [b]
[a] Tenneco Automotive Eastern Europe, Eastern European Engineering Center (EEEC), Control and Measuring Systems Department,
ul. Bojkowska 59b, 44-100 Gliwice, Poland
[b] Division of Mechatronics and Designing of Technical Systems,
Institute of Engineering Processes Automation and Integrated Manufacturing Systems,
Silesian University of Technology, ul. Konarskiego 18a, 44-100 Gliwice, Poland
* Corresponding author: E-mail address: piotr.czop@tenneco.com

Received 06.02.2009; published in revised form 01.04.2009

Analysis and modelling

ABSTRACT

Purpose: The aim of this paper is to develop a model of a valve system applicable for strain and stress prediction.
Design/methodology/approach: The analytical and numerical approaches are presented to provide an overview for available methods and prediction accuracy.
Findings: An equivalent numerical model of a disc valve system of different complexity was developed and discussed.
Research limitations/implications: It is important to provide a model functionality allowing for calculation of disc stacks supported by a coil spring and stack settings having the opening limiter. Disc stack stress and opening characteristics vs. applied pressure may be determined with simplified analytically derived model and full 2D model including almost all significant forces and moments in a stack of circular plates. An advantage of a simplified disc stack model is possibility of its implementation in an environment supporting matrix operations, e.g. Matlab.
Practical implications: A valve system has to withstand the cyclic pressure load across the piston. The number of discs, their diameters and thicknesses directly affect durability of a valve system. Damper force and valve durability expressed in life-cycles are the optimization criteria considering during selection and tuning of a valve system.
Originality/value: A new valve system was developed in two versions, i.e. simplified and advanced. The model allows durability prediction at the design stage reducing the testing costs of low-performance valve systems.
Keywords: Computational mechanics; Finite Elements Model; Valve system; Shock absorber

Reference to this paper should be given in the following way:
P. Czop, D. Sławik, P. Śliwa, G. Wszołek, Simplified and advanced models of a valve system used in shock absorbers, Journal of Achievements in Materials and Manufacturing Engineering 33/2 (2009) 173-180.

1. Introduction

Within recent years the subject of durability has increased in importance for two reasons. Firstly, unquestionable growth in quality demands in the automotive sector caused the warranty period requirements to be significantly prolonged and there is a clear tendency towards lowering the shock absorbers fatigue failures. Secondly, in the 1980s the first computer controlled variable damping systems were introduced to the passenger car market. These systems are quite complex mechatronics devices requiring trade off between durability, performance and tunability.

Therefore, engineers, with the aid of continuously broadening knowledge and increasing computational power, improved the performance of their designs making better use of limited resources, e.g. human resources, available materials and testing capacity.

There are two types of tests for valve system validation, i.e. static and dynamic. The static test is performed on a precise load frame machine whilst the dynamic test is performed on a hydraulic testing machine equipped with a high frequency hydraulic actuator. The objective of a static test is to determine a force-displacement characteristic. A dynamic test is intended to evaluate the trend of force or displacement vs. valve system lifetime to compose the Wöhler curve under accelerated damage conditions (Fig. 1).

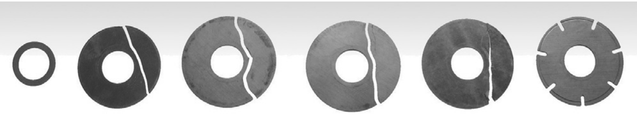

Fig. 1. Fatigue failure of a disc stack

Intensive development of analytical tools aimed at fatigue wear prediction was initiated in Tenneco in the 1980s.

The majority of the implemented improvements have gradually been introduced into practice. Before the invention of a personal computer, calculations required for the valve systems prediction were, in many cases, too time consuming and prone to error to be practical. The early prediction methods involved Roark's stress and strain formulas stated in the form of the pre-derived and parameterized equations [1]. Fundamentals of the disc stack prediction and the interpretation of the fatigue wear process were deduced from theoretical studies [2, 3, 4, 5, 6, 7, 8, 9, 10] and adapted to prototypical and manufactured valve systems [11, 12]. During two decades, existing approaches to valve system modeling and measurement data interpretation are being continually improved [2] and a finite element modeling approach is being implemented and supports development of more advanced models [13, 14]. Nowadays, the use of powerful workstations allows more complex algorithms, including a multi-variant sensitivity analysis, measurement data analysis and model-driven design, to be employed in design process. It is possible to develop a valve system pre-selection method based on simulation results that facilitates lowering required testing capacity, i.e. the number of long-term and expensive durability tests performed on hydraulic testing machines. On the other hand sophisticated finite element models of valve systems are developed to optimize and improve understanding of their operation. Owing to the potential for higher model performance, special attention is currently being paid to model validation. Available laboratory testing equipment allows for the correlation of the measurement and simulation results to be obtained. It is important to provide effective feedback for further research and development-oriented work.

2. Valve system models

This section discusses three types of valve system models. These are simplified linear (Matlab), simplified nonlinear (Matlab) and advanced non-linear (Abaqus) models. Model simplification refers to geometrical model representation. A simplified disc stack model assumes flexural rigidity assigned to annular finite elements. The most general discretization is provided through application of a grid of finite elements in an advanced model created utilizing a general-purpose software package Abaqus. Results of simulations performed with the advanced model take into account influence of a valve assembly.

2.1. Linear model

Simplified linear model considers only the essential functionality of a valve system, i.e. a hub determining the clamping diameter as a rigid element, discs of different diameters and thicknesses, uniform pressure load or force and a land limiting the area to which pressure is applied (Fig. 2).

A disc is divided into a set of finite elements having a shape of narrow annular elements with fixed length and thickness (Fig. 3). It is assumed that the force is acting on the right hand side of annular finite element (Fig. 3). This assumption is needed to fix radius R_{i+1} as constant R and radius R_i as variable r

$$R_i = r, \qquad R_{i+1} = R = \text{const} \tag{1}$$

Distribution of the force F over a circle of radius R of an annular finite element is given by

$$2\pi R Q_F = F \Rightarrow Q_F = \frac{F}{2\pi R} \tag{2}$$

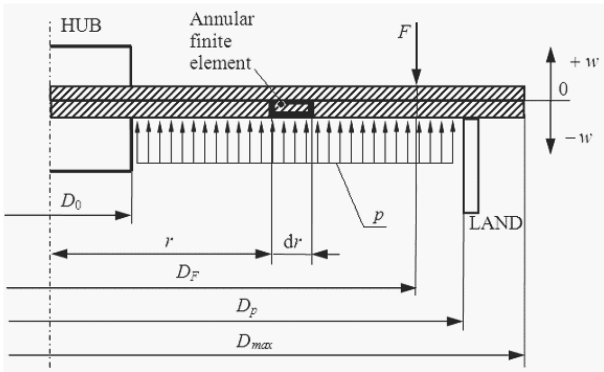

Fig. 2. Geometry and load distribution layout (D_0 – clamping diameter [m], D_F – diameter of applied force [N], D_p – land (hydraulic) diameter [m], D_{max} – maximal diameter of disc stack [m], F – load force [N], p – load pressure [Pa], r – polar coordinate of finite element, w – vertical deflection [m])

The pressure is acting on the right hand side of the annular finite element (Fig. 3) is responsible for creating force

$$F_p = p \cdot \pi (R_p^2 - r^2) \tag{3}$$

where $R_p = \frac{1}{2} D_p$. Distribution of the force F_p over a circle of radius R of the annular finite element is given by the formula

$$2\pi R Q_p = F_p,$$

$$Q_p = \frac{F_p}{2\pi R} = \frac{p(R_p^2 - r^2)}{2R} \tag{4}$$

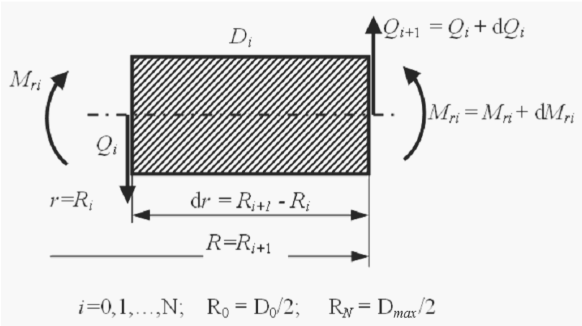

Fig. 3. Annular finite element

The resultant load is the sum of the pressure and force load

$$Q = Q_F + Q_P \tag{5}$$

The right hand side of pure bending equation [15] can be rewritten in a form explicitly referring to the load conditions given by (5) (where *D* is a flexural rigidity of a disc and *F* is a load force applied to the disc)

$$\frac{d}{dr}\left[\frac{1}{r}\frac{d}{dr}\left(r\frac{dw}{dr}\right)\right] = \frac{Q}{D} = A + BR_p^2 - Br^2 \tag{6}$$

with constants

$$A = \frac{F}{2\pi RD}, \quad B = \frac{p}{2RD} \tag{7}$$

Integrating equation (6) and multiplying by r one obtains

$$\frac{d}{dr}\left(r\frac{dw}{dr}\right) = Ar^2 + BR_p^2 r^2 - \frac{1}{3}Br^4 + C_1 r \tag{8}$$

Integrating again one has

$$r\frac{dw}{dr} = \frac{1}{3}Ar^3 + \frac{1}{3}BR_p^2 r^3 - \\ -\frac{1}{15}Br^5 + \frac{1}{2}C_1 r^2 + C_2 \tag{9}$$

Dividing both sides of (9) by r gives the disc slope

$$\frac{dw}{dr} = \frac{1}{3}Ar^2 + \frac{1}{3}BR_p^2 r^2 - \\ -\frac{1}{15}Br^4 + \frac{1}{2}C_1 r + C_2\frac{1}{r} \tag{10}$$

Third integration gives the disc deflection w

$$w = \frac{1}{9}Ar^3 + \frac{1}{9}BR_p^2 r^3 - \frac{1}{75}Br^5 + \\ +\frac{1}{4}C_1 r^2 + C_2\ln(r) + C_3 \tag{11}$$

The radial moment is determined by differentiating equation (10) thus obtaining

$$\frac{d^2 w}{dr^2} = \frac{2}{3}Ar + \frac{2}{3}BR_p^2 r - \\ -\frac{4}{15}Br^3 + \frac{1}{2}C_1 - C_2\frac{1}{r^2} \tag{12}$$

Radial moment M_r is obtained by substituting equations (10) and (12) to equation of bending moments [15]

$$M_r = -\left[\frac{1}{3}Ar(2+\nu) + \frac{1}{3}BR_p^2 r(2+\nu) - \\ -\frac{1}{15}Br^3(4+\nu) + \frac{1}{2}C_1(1+\nu) + C_2\frac{1}{r^2}(-1+\nu)\right] \tag{13}$$

Finally, from equations (7) obtained are:
(i) the deflection w

$$w(r) = \frac{1}{9}\frac{F}{2\pi RD}r^3 + \frac{1}{9}\frac{p}{2RD}R_p^2 r^3 - \\ -\frac{1}{75}\frac{p}{2RD}r^5 + \frac{1}{4}C_1 r^2 + C_2\ln(r) + C_3 \tag{14}$$

(ii) the slope dw/dr

$$\frac{dw(r)}{dr} = \frac{1}{3}\frac{F}{2\pi RD}r^2 + \frac{1}{3}\frac{p}{2RD}R_p^2 r^2 - \\ -\frac{1}{15}\frac{p}{2RD}r^4 + \frac{1}{2}C_1 r + C_2\frac{1}{r} \tag{15}$$

(iii) the radial moment M_r

$$M_r(r) = -D\left[\frac{1}{3}\frac{F}{2\pi RD}r(2+\nu) + \\ +\frac{1}{3}\frac{p}{2RD}R_p^2 r(2+\nu) - \frac{1}{15}\frac{p}{2RD}r^3(4+\nu) + \\ +\frac{1}{2}C_1(1+\nu) + C_2\frac{1}{r^2}(-1+\nu)\right] \tag{16}$$

Taking into account equations (14), (15) and (16), the annular finite elements (Fig. 3) are described by the following formulas

$$w_i(r) = \frac{1}{9}\frac{F_i}{2\pi R_{i+1}D_i}r^3 + \frac{1}{9}\frac{p_i}{2R_{i+1}D_i}R_p^2 r^3 - \\ -\frac{1}{75}\frac{p_i}{2R_{i+1}D_i}r^5 + \frac{1}{4}C_{1,i}r^2 + C_{2,i}\ln(r) + C_{3,i} \tag{17}$$

$$\frac{dw_i(r)}{dr} = \frac{1}{3}\frac{F_i}{2\pi R_{i+1}D_i}r^2 + \frac{1}{3}\frac{p_i}{2R_{i+1}D_i}R_p^2 r^2 - \\ -\frac{1}{15}\frac{p_i}{2R_{i+1}D_i}r^4 + \frac{1}{2}C_{1,i}r + C_{2,i}\frac{1}{r} \tag{18}$$

$$M_{r,i}(r) = -D\left[\frac{1}{3}\frac{F_i}{2\pi R_{i+1}D_i}r(2+\nu) + \\ +\frac{1}{3}\frac{p_i}{2R_{i+1}D_i}R_p^2 r(2+\nu) + \dots \quad \dots - \\ -\frac{1}{15}\frac{p_i}{2R_{i+1}D_i}r^3(4+\nu) + \\ +\frac{1}{2}C_{1,i}(1+\nu) + C_{2,i}\frac{1}{r^2}(-1+\nu)\right] \tag{19}$$

where

$$F_i = \begin{cases} F & if \quad r \le \tfrac{1}{2} D_F \\ 0 & if \quad r < \tfrac{1}{2} D_F \end{cases} \tag{20}$$

and

$$p_i = \begin{cases} p & if \quad r \le \tfrac{1}{2} D_p \\ 0 & if \quad r < \tfrac{1}{2} D_p \end{cases} \tag{21}$$

Equations are supplemented with boundary conditions:

(i) the deflection w of element no. 0 at the clamping diameter R_0 is equal to zero

$$w_0(r)\big|_{r=R_0} = 0 \tag{22}$$

(ii) the slope dw/dr of element no. 0 at the clamping diameter R_0 is equal to zero

$$\left.\frac{dw_0}{dr}\right|_{r=R_0} = 0 \tag{23}$$

(iii) the radial moment M_r of element no. N at the disc edge (diameter D_{max}) is equal to zero

$$M_{r,N}(r)\big|_{r=D_{max}/2} = 0 \tag{24}$$

(iv) the deflection w at the end of ith finite element and deflection w at the start of (i+1)th finite element are equal

$$w_i(r)\big|_{r=R_{i+1}} = w_{i+1}(r)\big|_{r=R_{i+1}} \tag{25}$$

(v) the slope dw/dr at the end of ith finite element end slope dw/dr at the start of (i+1)th finite element are equal

$$\left.\frac{dw_i}{dr}\right|_{r=R_{i+1}} = \left.\frac{dw_{i+1}}{dr}\right|_{r=R_{i+1}} \tag{26}$$

(vi) the radial M_r at the end of ith finite element end radial moment M_r at the start of (i+1)th finite element are equal

$$M_{r,i}(r)\big|_{r=R_{i+1}} = M_{r,i+1}(r)\big|_{r=R_{i+1}} \tag{27}$$

Equations of the simplified model have been implemented in Matlab so that their solutions can be presented in a graphical and text form.

2.2. Nonlinear model

The nonlinear model is an extension of the linear one [16]. The nonlinear model takes into account two variables, radial and perpendicular strains as discussed in sec. 2. Equations above are rewritten as a system of five first-order differential equations [17]. At each transition between finite annular elements, the value of the actual curvature and radial strain needs to reflect the equivalent thickness change.

The first constraint (28) results from the equality of moment while the second (29) results from the equality of force. The displacement, slope and radial displacement are unchanged at each transition. This system of equations can be solved for the set of given initial conditions, i.e. displacement, slope, curvature, radial displacement and strain at the clamping radius. For a rigid clamping the displacement and the radial displacement are both equal 0 by definition. The slope is known and defined by the piston geometrical relations. Two other initial conditions are unknown and have to be found iteratively using the linear model to improve the accuracy of the initial guess. Such an approach was first proposed in [16].

$$\begin{aligned} \left.\frac{d^2 w}{dr^2}\right._{i+1} &= -\left(\frac{v}{r}\frac{dw}{dr}\right) + \\ &+ \frac{D_i}{D_{i+1}}\left[\left.\frac{du}{dr}\right._i + \frac{v \cdot u}{r} + \frac{1}{2}\left(\frac{dw}{dr}\right)\right] \end{aligned} \tag{28}$$

$$\begin{aligned} \left.\frac{du}{dr}\right._{i+1} &= -\frac{1}{2}\left(\frac{dw}{dr}\right)^2 - \frac{v \cdot u}{r} + \\ &+ \frac{t_i}{t_{i+1}}\left[\left.\frac{du}{dr}\right._i + \frac{1}{2}\left(\frac{dw}{dr}\right)^2 + \frac{v \cdot u}{r}\right] \end{aligned} \tag{29}$$

2.3. Advanced nonlinear model

An advanced valve system model takes two forms depending on the symmetry of the system. A two-dimensional (2D) geometrical discretization with a four-node (quadrilateral - Abaqus CAX4I) finite elements mesh is used when the system is axisymmetrical while a fully three-dimensional (3D) mesh (linear hexahedral - Abaqus C3D8R) in all the other cases Fig. 4. At least four finite elements create the disc thickness. The advanced model requires implementation of a checking routine ensuring equality of the applied and reaction forces and moments. In case of nonconvergence during the simulation, a small amount of additional energy, the so called stabilization energy, is artificially added. Based on experience it was decided that the stabilization energy shall never exceed 5% of the energy already stored in the system.

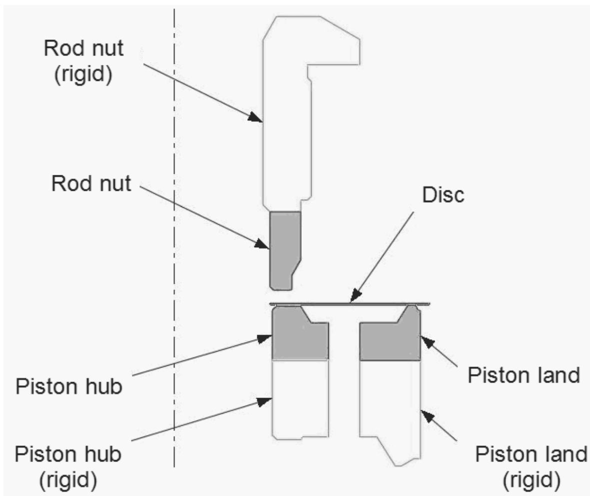

Fig. 4. Finite element model geometry and parts

Standard model for pressure-force load

There are three steps essential to load and unload a disc stack in a model: applying preload, applying and then releasing pressure load. During the preload step, the rod nut (rigid) is moved down, while the piston hub (rigid) and land (rigid) are held fixed. The nut moves until the clamping force is equal to the specified preload force. In the next step, the pressure or additional force load is applied to the disc. In the last step, the pressure applied to the disc in the previous step is released. Part names and designation "rigid" refers to Fig. 4.

Bending tool model for displacement-force load

In this case, the first step is the same. During the preload step, the rod nut (rigid) is moved down, while the piston hub (rigid) and land (rigid) are held fixed. The nut moves until the clamping force is equal to the specified preload force. In the next step, the displacement is applied to the piston land (rigid) while the relative position of the rod nut (rigid) and the piston hub (rigid) is fixed. In the last step, the displacement applied to the piston land (rigid) in the previous step is released. Part names and designation "rigid" refers to Fig. 4.

3. Model benchmarking under pressure load

Models described in previous sub-sections allow flexible customization of disc stack computations depending on the simulation purpose and available lead time. The models were ranked regarding their functionality in Table 1.

Table 1.
Comparison of properties of valve system models

Model properties	Linear simplified model	Nonlinear simplified model	Advanced model
Disc clamping	rigid	rigid	elastic/ rigid
Land material	rigid	rigid	elastic/ rigid
External friction	no	no	yes
Back pressure	yes	no	yes
Plasticity	no	no	yes
Pressure load distribution	uniform	uniform /arbitrary	uniform /arbitrary
Disc material parameters	same for each disc	same for each disc	may be different for each disc
Simulation time	<5 sec	<2min	2D: <3h; 3D: <16h
Travel stop	no	no	yes
Discs contact imperfections	no	no	yes

The simplified linear and nonlinear models were compared to advanced model for the same set of the input parameters called setting S-I and setting S-II (Table 2). Configuration of both settings is given in Table 3.

Table 2.
Simulation parameters

No.	Parameter name	Symbol	Unit	Value
1	Poisson's ratio	ν	-	0.30
2	Young's Modulus	E	MPa	2.1e5
3	Disc thickness	h	mm	In tab. 3
4	Outer disc diameter	D_{max}	mm	In tab. 3
5	Land (hydraulic) diameter	D_p	mm	24.64
6	Clamping diameter	D_0	mm	12.30
7	Pressure	p	bar	50.00
8	Force radius	R_0	mm	24.65
9	Force value	F	N	see
10	Length of finite element	dr	mm	0.01

Table 3.
Disc stack setting configuration

Setting type	Discs used in a stack
S-I	B
S-II	A, B, C, D, E, F and G

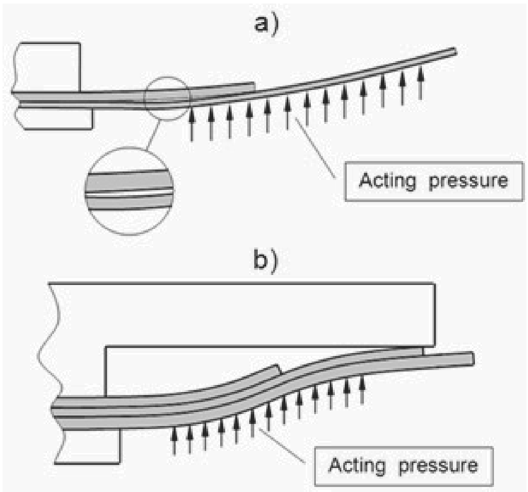

Fig. 5. Disc stack with: a) small gap between discs; b) disc displacement limitation

A pressure load, being a typical simulation case, has been used for benchmarking. Properties of the models are described in the Table 1 as a list of features taken into account in a particular model. The disc clamping is the flexible fixation of discs using the specified torque applied at the rod nut (Fig. 4). An elastic land material model provides more realistic contact model between a disc and its supporting edge. External friction model allows for quantifying the influence of the external disc friction in case of multi disc stacks. Using the backpressure property makes it possible to apply the load on the opposite side of the disc stack.

The backpressure may be a reason of disc stack failure. In turn, the plasticity property allows for testing the valve system model beyond the Hook's low applicability. The pressure load distribution property defines a nonuniform pressure distribution over the disc surface. This property is used for atypical designs, for instance for designs in which slots passing the oil to valve interior are very narrow focusing the fluid pressure at a specific part of a disc. In case of customized simulations, different material properties for each disc may be specified in the advanced model. A disc travel stop is commonly implemented to limit the maximal stress level. This property is crucial in realistic reproduction of valve opening movement and reliable stress prediction. The presence of a disc opening end stop affects model prediction qualitatively (Fig. 5b). Discs contact imperfections are taken into account only in the advanced model (Fig. 5a). It is recommended to use the non-axisymmetrical model when the valve has irregular lands, e.g. in the form of islands.

In case of a simplified linear model, the benchmarking simulation results indicate that the force error amounts to approximately 100% when the displacement is equal to the half of the thickness of the thinnest disc in a stack (Fig. 6, 7). Despite such a large error, the simplified model is useful for understanding the physics behind the disc stack operation and compare disc stack relatively to each other. The simplified nonlinear model predicts the strain sufficiently accurately. The small difference is expected since the simplified model ignores important aspects, like elastic disc clamping, disc travel stop and geometrical imperfections, of the valve system functionality. Rigid clamping of a disc stack is the most significant contribution to the strain overestimation.

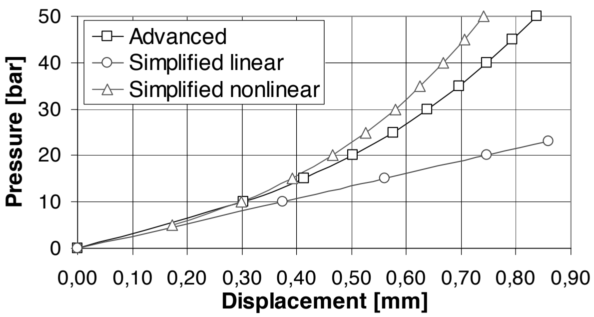

Fig. 6. Comparison of the simplified linear/nonlinear model and advanced model for setting S-I (Table 3)

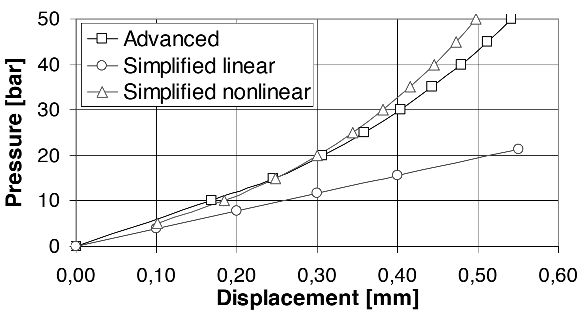

Fig. 7. Comparison of the simplified linear/nonlinear model and advanced model for setting S-II (Table 3)

The disc stress on any given surface area element can be decomposed into two parts: a normal component acting in the direction perpendicular to the stressed surface [18] and a shear component, acting in the direction parallel to the stressed surface. A scalar Mises stress value can be determined from the stress tensor in the following way

$$\sigma_M = \sqrt{\tfrac{3}{2}\{[\sigma_{11} - \tfrac{1}{3}(\sigma_{11}+\sigma_{22}+\sigma_{33})]^2 + [\sigma_{22} - \tfrac{1}{3}(\sigma_{11}+\sigma_{22}+\sigma_{33})]^2 + [\sigma_{33} - \tfrac{1}{3}(\sigma_{11}+\sigma_{22}+\sigma_{33})]^2 + \tau_{12}^2+\tau_{13}^2+\tau_{21}^2+\tau_{23}^2+\tau_{31}^2+\tau_{32}^2\}} \quad (30)$$

For the particular case [15], the Mises stress formula (30) can be simplified to the form

$$\sigma_C = \sqrt{\tfrac{3}{2}\{[\sigma_{11} - \tfrac{1}{3}(\sigma_{11}+\sigma_{22}+\sigma_{33})]^2 + [\sigma_{22} - \tfrac{1}{3}(\sigma_{11}+\sigma_{22}+\sigma_{33})]^2 + [\sigma_{33} - \tfrac{1}{3}(\sigma_{11}+\sigma_{22}+\sigma_{33})]^2 + \tau_{12}^2\}} \quad (31)$$

In the simplified linear or nonlinear model, the share stresses in formula (46) are neglected further simplifying the Mises stress formula as follows

$$\sigma_C = \sqrt{\sigma_{11}^2 + \tau_{12}^2} \quad (32)$$

The shear stress is negligible compared to normal stress. The stress at the center and at the edge of the plate in the radial direction can be obtained as the sum of the membrane stress and the bending stress

$$\sigma_C = \frac{N_r}{h} + \frac{6M_r}{h^2} \quad (33)$$

The stress values computed by the model are presented in the Table 4 and Table 5.

Table 4.
Stress values obtained for 5 bar pressure (setting S-I)

Disc	Advanced model [MPa]	Simplified linear model [MPa]	Simplified nonlinear model [MPa]
B	870.0	870.5	435.2

Table 5.
Stress values obtained for 5 bar pressure (setting S-II)

Disc	Advanced model [MPa]	Simplified linear model [MPa]	Simplified nonlinear model [MPa]
A	146.00	146.09	73.04
B	438.00	438.28	219.14
C	292.00	292.19	146.09
D	219.00	219.14	109.57
E	219.00	219.14	109.57
F	219.00	219.14	109.57
G	292.00	292.19	146.09

The simulations were performed for settings consisting of discs as specified in Table 3 and Table 6.

Table 6.
Geometrical properties of the discs

Disc type	Inner diameter [mm]	Outer diameter [mm]	Thickness [mm]
Disc A	9.600	27.000	0.100
Disc B	9.600	27.000	0.300
Disc C	9.600	13.500	0.200
Disc D	9.600	20.000	0.150
disc E	9.600	24.525	0.150
disc F	9.600	27.000	0.150
Disc G	9.600	27.000	0.200

Nomenclature

D	– flexural rigidity of a disc [Pa·m^3]
D_0	– clamping diameter [m]
D_F	– diameter of applied force [N]
D_{max}	– maximal diameter of disc stack [m]
D_p	– land (hydraulic) diameter [m]
dr	– length of finite element [mm]
E	– Young modulus [Pa]
F	– load force [N]
h	– disc thickness [mm]
M_r	– radial bending moment [N·m]
N_r	– radial directional vector [N/m]
p	– load pressure [Pa]
Q	– applied shear force [N]
Q_F	– applied shear force corresponding to load force [N]
Q_p	– applied shear force corresponding to load pressure [N]
r	– polar coordinate of finite element
R	– radius (constant) [m]
R_0	– force radius [mm]
R_p	– external radius of applied pressure [m]
w	– vertical deflection [m]
ν	– Poisson ratio (ν = 0.3)
σ_c	– compound stresses [Pa]
σ_M	– stress tensor [Pa]
σ_{11}	– direct (normal) stress in the 1-direction (in the x axis direction)
σ_{22}	– direct (normal) stress in the 2-direction (in the y axis direction)
σ_{33}	– direct (normal) stress in the 3-direction (in the z axis direction)
τ_{12}	– shear stress in the 1,2-plane (in the plane defined with x and y axis)

4. Conclusions

Expertise available within engineering staff may be captured in a model and utilized to optimize the behavior of a valve system. The paper covers numerical verification of an equivalent model of a disc-spring valve system widely used in automotive shock absorbers. Two valve system models have been considered and built. These models are referred to as simplified and advanced. The simplified model is stated in an explicit form as a set of equations derived using bending theory of circular plates for small and large plate deflections, respectively [17]. A number of assumptions underlying this approach justifies calling the model "simplified". The simplified model may be applied to shock absorber models if a system approach is considered and results have to be obtained within a restricted time horizon. In turn, the advanced model has been developed using finite element approach and implemented in the Abaqus software. The advanced model focuses mainly on detailed modeling of mechanical properties of a valve system in order to properly evaluate stress. In addition, this model takes into account contributions of components supporting the disc stack, even under complex load distributions.

References

[1] W.C. Young, Roark's Formulas for Stress and Strain, McGraw-Hill, 2003.

[2] Y. Lee, J. Pan, R. Hathaway, M. Barkey, Fatigue testing and analysis, Elsevier Inc., Oxford, 2005

[3] J. N. Reddy, Theory and Analysis of Elastic Plates, Taylor & Francis, 1999.

[4] L. M. Kachanov, Fundamentals of the Theory of Plasticity, Courier Dover Publications, 2004.

[5] J. P. Den Hartog, Advanced Strength of Materials, Courier Dover Publications, 1987.

[6] J. Chakrabarty, Applied Plasticity, Springer, 2000.

[7] K. Chandrashekhara, Theory of Plates, Orient Longman, 2001.

[8] E. Ventsel, T. Krauthammer, Thin Plates and Shells: Theory, Analysis, and Applications, CRC Press, 2001.

[9] E. Bayraktar, J. Masounave, R. Caplain, C. Bathias, Manufacturing and damage mechanisms in metal matrix composites, Journal of Achievements in Materials and Manufacturing Engineering 31/1 (2008) 294-300.

[10] H. Imrek, M. Bagci, O.M. Khalfan, Experimental investigation of effects of external loads on erosive wear, Journal of Achievements in Materials and Manufacturing Engineering 32/1 (2009) 18-22.

[11] S. Duym, S. Dupont, D. Coppens, Data Reduction of Durability Tests for Shock Absorbers, 23rd International Seminar on Modal Analysis, Leuven, Belgium (1998) 217-225.

[12] A.W. Leissa, Vibration of Plates, Ohio State University, Scientific and Technical Information Division, Washington, D.C., 1969.

[13] U. Suripa A. Chaikittiratana, Finite element stress and strain analysis of a solid tyre, Journal of Achievements in Materials and Manufacturing Engineering 31/1 (2008) 576-579.

[14] C.L. Chang, S.H. Yang, Finite element simulation of wheel impact test, Journal of Achievements in Materials and Manufacturing Engineering 28/1 (2008) 167-170.
[15] P. Czop, D. Sławik, P. Śliwa, G. Wszołek, Circular plates theory applied to modeling of intake valves used in shock absorbers, Journal of Achievements in Materials and Manufacturing Engineering (2009) (in print).
[16] X. Lauwerys, Nonlinear disc stack model for valve design, Intercompany test and analysis report, Tenneco Automotive, 1998.
[17] S.P. Timoshenko, S. Woinowsky-Krieger, Theory of Plates and Shells, McGraw-Hill Kogakusha Ltd., 2nd edition, 1959.
[18] Abaqus PDF Documentation v6.7, Dassault Systèmes, 2007.